Off-resonant dielectronic recombination in a collision of an electron with a heavy hydrogenlike ion

Vladimir A. Yerokhin[1,2,3] and Andrey Surzhykov[1,2]

[1]*Institute of Physics, University of Heidelberg, Philosophenweg 12, D-69120 Heidelberg, Germany*

[2]*Gesellschaft für Schwerionenforschung, Planckstraße 1, D-64291 Darmstadt, Germany*

[3]*Center for Advanced Studies, St. Petersburg State Polytechnical University, Polytekhnicheskaya 29, St. Petersburg 195251, Russia*

(Received 3 May 2010; published 8 June 2010)

The recombination of an electron with an (initially) hydrogenlike ion is investigated. The effect of the electron-electron interaction is treated rigorously to the first order in the parameter $1/Z$ and within the screening-potential approximation to higher orders in $1/Z$, with Z being the nuclear charge number. The two-electron correction contains the dielectronic recombination part, which contributes to the process not only under the resonance condition for the projectile energy but also in the regions far from resonances. The mechanism of the off-resonant dielectronic recombination is studied in detail.

DOI: 10.1103/PhysRevA.81.062703 PACS number(s): 34.80.Lx, 34.10.+x, 31.30.jc

I. INTRODUCTION

One of the main processes occurring in collisions of a highly charged ion with an electron is radiative recombination (RR), in which the electron is captured from the continuum into a bound state with emission of a photon. In the case when the ion initially possesses one or several electrons, the electron capture can proceed also via dielectronic recombination (DR), in which the energy excess goes to the excitation of the second electron, which then returns to the ground state via a radiative decay. DR is a resonant process and is usually studied under the condition that the excess energy is very close to the excitation energy of the second electron. In this case, DR is the dominant recombination channel, whereas RR is responsible for a nonresonant background. Outside of the resonance region, RR is the dominant process.

In the zero-order approximation, RR and DR are often considered to be two independent recombination channels, which can be calculated separately and combined additively [1]. More accurate calculations include the effects of quantum interference between DR and RR [2–4]. Generally speaking, at the level of precision where effects of the electron-electron interaction come into play, RR and DR cannot be meaningfully separated. Outside of the resonance region, DR is essentially a correction to RR due to the electron-electron interaction and induces a contribution of the same order of magnitude as other two-body effects [e.g., the screening of the nuclear charge by core electron(s)].

The accuracy of experimental investigations of the RR process with heavy highly charged ions has gradually increased during the past years [5–7], reaching a level at which the electron-electron interaction effect can be clearly identified [8]. A disagreement with the one-electron theory observed in the state-selective study of RR into hydrogenlike uranium [8] calls for an accurate theoretical description of the electron-electron interaction effect.

Most of the previous calculations of the RR process into heavy few-electron ions accounted for the electron correlation by means of the Dirac-Fock method [9,10], disregarding the off-resonant DR mechanism. Evidence that the omitted contribution might be significant was reported in Refs. [11,12], where a part of the off-resonant DR (involving photon emission from a core electron) was studied. It was claimed that, for many-electron systems, this mechanism can significantly influence the RR process, yielding an order-of-magnitude enhancement in some specific cases.

In the present investigation we perform an *ab initio* calculation of the electron-electron interaction effect on RR into a heavy hydrogenlike ion in the nonresonant region of energies of the incoming electron. A particular emphasis is placed on the contribution of the off-resonant DR, as this effect has not been carefully studied before. A similar study of RR into a heliumlike uranium was reported previously in Ref. [13]. Relativistic units ($\hbar = c = 1$) are used in the present paper.

II. GENERAL APPROACH

We consider RR of an electron with an (initially) hydrogenlike ion. The initial state consists of the incident electron with the asymptotic momentum $\mathbf{p}$, the energy $\varepsilon = \sqrt{\mathbf{p}^2 + m^2}$, and the spin projection $\mu_s = \pm 1/2$ and the bound (core) electron in the state a' with relativistic angular quantum number $\kappa_{a'}$ and momentum projection $\mu_{a'}$. In the final state, there is the two-electron bound state with angular momentum J and projection M and the outgoing photon with momentum $\mathbf{k}$, and energy $\omega = |\mathbf{k}|$. The wave function of the final two-electron state is

$$|JM\rangle = N \sum_{\mu_a \mu_v} C^{JM}_{j_a \mu_a \, j_v \mu_v} |\kappa_a \mu_a\rangle |\kappa_v \mu_v\rangle \,, \tag{1}$$

where a and v stand for the core and the valence electron, respectively; $N = 1/\sqrt{2}$ for the equivalent electrons and $N = 1$ otherwise. The core electron state is not changed in the process; thus, $\kappa_a = \kappa_{a'}$. The wave function (1) is not antisymmetrized since we choose to perform antisymmetrization explicitly for the amplitude.

General formulas are conveniently written in the center-of-mass frame, which practically coincides with the rest system of the ion. The direction of the z axis of the coordinate system is chosen to be the direction of the emitted photon.

In the following, we assume that the fine-structure levels with different J's are *not* resolved in the experiment (as is the case for the experiments conducted so far).

A. Zero order

To zero order, we neglect the electron-electron interaction. The core electron does not participate in the process and the

transition amplitude is written as

$$\tau^{(0)}_{\mu_s\mu_{a'}JM} = N\sum_{\mu_a\mu_v} C^{JM}_{j_a\mu_a\, j_v\mu_v}\,\delta_{\mu_a\mu_{a'}}\,\tau^{(0)}_{\mu_s\mu_v}, \tag{2}$$

where $\tau^{(0)}_{\mu_s\mu_v}$ is the amplitude for the recombination with the bare nucleus. It reads [14]

$$\tau^{(0)}_{\mu_s\mu_v} = \langle v|\boldsymbol{\alpha}\cdot\hat{\mathbf{u}}^* e^{-i\mathbf{k}\cdot\mathbf{r}}|p\rangle, \tag{3}$$

where $|v\rangle \equiv |\kappa_v\mu_v\rangle$ denotes the bound state, $|p\rangle \equiv |\mathbf{p}\mu_s\rangle$ is the Dirac continuum-state wave function with a definite asymptotic momentum, and $\hat{\mathbf{u}}$ is the unit polarization vector of the emitted photon. After summation over the final states and averaging over the initial states, the differential cross section of the process is written as

$$\frac{d\sigma^{(0)}}{d\Omega} = \frac{1}{2j_a+1}\frac{\alpha\omega m}{4\beta^2\varepsilon^2}\sum_{\mu_s\mu_{a'}JM}\left|\tau^{(0)}_{\mu_s\mu_{a'}JM}\right|^2 = N^2\frac{\alpha\omega m}{4\beta^2\varepsilon^2}\sum_{\mu_s\mu_v}\left|\tau^{(0)}_{\mu_s\mu_v}\right|^2, \tag{4}$$

where $\beta = \sqrt{1-m^2/\varepsilon^2}$. Because of the summation over the initial and final states, the cross section does not depend on the polarization of the emitted photon, which can be fixed arbitrarily. The formula (4) differs from the corresponding expression for the RR into the bare nucleus [14] only by a factor of N^2 ($=1/2$ for the recombination into the ground state and 1 otherwise).

The energy of the emitted photon in Eq. (4) is fixed by the energy conservation condition $\omega = \varepsilon - \varepsilon_v$ or, more generally, $\omega = \varepsilon - m + \varepsilon_{\rm io}$, where $\varepsilon_{\rm io}$ is the ionization energy of the atom in the final state.

B. Electron-electron interaction

For a heavy few-electron ion, the electron-electron interaction can be effectively accounted for by a perturbative expansion in the parameter $1/Z$. The first-order correction is induced by a single virtual-photon exchange between the electrons, shown diagrammatically in Fig. 1. The corresponding correction to the differential cross section can be written as

$$\frac{d\sigma^{(1)}}{d\Omega} = \delta_\omega\frac{d\sigma^{(0)}}{d\Omega} + \frac{1}{2j_a+1}\frac{\alpha\omega m}{4\beta^2\varepsilon^2} \times \sum_{\mu_s\mu_{a'}JM} 2\,\mathrm{Re}\left[\tau^{(0)*}_{\mu_s\mu_{a'}JM}\tau^{(1)}_{\mu_s\mu_{a'}JM}\right], \tag{5}$$

where $\tau^{(1)}$ denotes the first-order correction to the amplitude and δ_ω is induced by the change of the energy of the emitted photon (because of the shift of the energy of the final state due to the presence of the second electron),

$$\delta_\omega\frac{d\sigma^{(0)}}{d\Omega} = \left.\frac{d\sigma^{(0)}}{d\Omega}\right|_{\omega=\omega^{(0)}+\delta\omega} - \left.\frac{d\sigma^{(0)}}{d\Omega}\right|_{\omega=\omega^{(0)}}. \tag{6}$$

We note that Eq. (5) assumes that the perturbative regime ($|\tau^{(1)}| \ll |\tau^{(0)}|$) takes place.

Since the fine-structure sublevels of the final state are not resolved in the experiment, the dependence on J and M can be eliminated already in the general formulas. To achieve this, we write the correction to the amplitude as

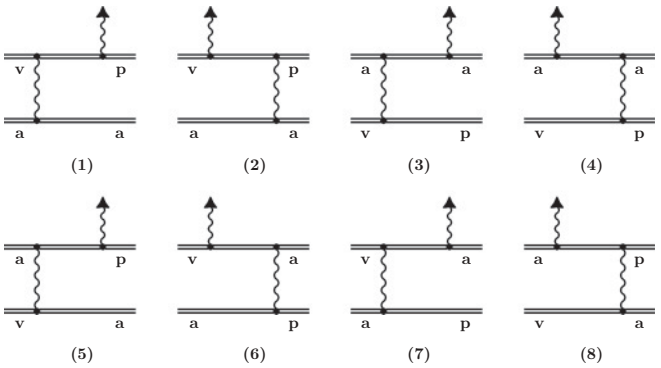

FIG. 1. The one-photon exchange correction to the transition amplitude of the radiative recombination of an electron with a hydrogenlike ion. The double line indicates an electron propagating in the field of a nucleus. The wavy line with an arrow denotes the emitted photon. The incoming electron is denoted as p, a is the initially bound (core) electron, and v is the captured (valence) electron.

$$\tau^{(1)}_{\mu_s\mu_{a'}JM} = N\sum_{\mu_a\mu_v} C^{JM}_{j_a\mu_a\, j_v\mu_v}\,\tau^{(1)}_{\mu_s\mu_{a'}\mu_v\mu_a}, \tag{7}$$

where $\tau^{(1)}_{\mu_s\mu_{a'}\mu_v\mu_a}$ does not depend on J and M. Inserting this formula and Eq. (2) into Eq. (5) and performing summations, we obtain

$$\frac{d\sigma^{(1)}}{d\Omega} = \delta_\omega\frac{d\sigma^{(0)}}{d\Omega} + \frac{N^2}{2j_a+1}\frac{\alpha\omega m}{4\beta^2\varepsilon^2}\sum_{\mu_s\mu_v} 2\,\mathrm{Re}\left[\tau^{(0)*}_{\mu_s\mu_v}\tau^{(1)}_{\mu_s\mu_v}\right]. \tag{8}$$

Here,

$$\tau^{(1)}_{\mu_s\mu_v} \equiv \sum_{\mu_a}\tau^{(1)}_{\mu_s\mu_a\mu_v\mu_a} \tag{9}$$

is the amplitude of the recombination with a closed-shell atom. So we obtain that, in the situation when the fine-structure levels are not resolved in the experiment, formulas for the RR with a hydrogenlike ion differ from those for the RR with a heliumlike ion only by a prefactor of $N^2/(2j_a+1)$.

General expressions for the one-photon exchange correction to the RR of an electron with a heavy ion were derived in Ref. [15]. (For the closed-shell ions, such a derivation was also reported in Ref. [13]). The correction to the transition amplitude consists of eight terms corresponding to the eight parts of Fig. 1,

$$\tau^{(1)}_{\mu_s\mu_v} = \sum_{i=1}^{8}\tau^{(1,i)}. \tag{10}$$

The individual contributions for each diagram are given by

$$\tau^{(1,1)} = \sum_{\mu_a}\sum_{n\neq v}\frac{\langle va|I(0)|na\rangle\langle n|\boldsymbol{\alpha}\cdot\hat{\mathbf{u}}^* e^{-i\mathbf{k}\cdot\mathbf{r}}|p\rangle}{\varepsilon_v-\varepsilon_n}, \tag{11}$$

$$\tau^{(1,2)} = \sum_{\mu_a}\sum_{n}\frac{\langle v|\boldsymbol{\alpha}\cdot\hat{\mathbf{u}}^* e^{-i\mathbf{k}\cdot\mathbf{r}}|n\rangle\langle na|I(0)|pa\rangle}{\varepsilon-\varepsilon_n(1-i0)}, \tag{12}$$

$$\tau^{(1,3)} = \sum_{\mu_a} \sum_{n} \frac{\langle va|I(\varepsilon-\varepsilon_v)|pn\rangle\langle n|\boldsymbol{\alpha}\cdot\hat{\mathbf{u}}^* e^{-i\mathbf{k}\cdot\mathbf{r}}|a\rangle}{\varepsilon_a+\varepsilon_v-\varepsilon-\varepsilon_n(1-i0)}, \quad (13)$$

$$\tau^{(1,4)} = \sum_{\mu_a} \sum_{n} \frac{\langle a|\boldsymbol{\alpha}\cdot\hat{\mathbf{u}}^* e^{-i\mathbf{k}\cdot\mathbf{r}}|n\rangle\langle vn|I(\varepsilon-\varepsilon_v)|pa\rangle}{\varepsilon_a-\varepsilon_v+\varepsilon-\varepsilon_n(1-i0)}, \quad (14)$$

$$\tau^{(1,5)} = -\sum_{\mu_a} \sum_{n\neq v} \frac{\langle av|I(\varepsilon_v-\varepsilon_a)|na\rangle\langle n|\boldsymbol{\alpha}\cdot\hat{\mathbf{u}}^* e^{-i\mathbf{k}\cdot\mathbf{r}}|p\rangle}{\varepsilon_v-\varepsilon_n} - \frac{1}{2}\sum_{\mu_a\mu_{v'}} \langle av|I'(\varepsilon_v-\varepsilon_a)|v'a\rangle\langle v'|\boldsymbol{\alpha}\cdot\hat{\mathbf{u}}^* e^{-i\mathbf{k}\cdot\mathbf{r}}|p\rangle, \quad (15)$$

$$\tau^{(1,6)} = -\sum_{\mu_a} \sum_{n} \frac{\langle v|\boldsymbol{\alpha}\cdot\hat{\mathbf{u}}^* e^{-i\mathbf{k}\cdot\mathbf{r}}|n\rangle\langle na|I(\varepsilon-\varepsilon_a)|ap\rangle}{\varepsilon-\varepsilon_n(1-i0)}, \quad (16)$$

$$\tau^{(1,7)} = -\sum_{\mu_a} \sum_{n} \frac{\langle av|I(\varepsilon-\varepsilon_a)|pn\rangle\langle n|\boldsymbol{\alpha}\cdot\hat{\mathbf{u}}^* e^{-i\mathbf{k}\cdot\mathbf{r}}|a\rangle}{\varepsilon_a+\varepsilon_v-\varepsilon-\varepsilon_n(1-i0)}, \quad (17)$$

$$\tau^{(1,8)} = -\sum_{\mu_a} \sum_{n} \frac{\langle a|\boldsymbol{\alpha}\cdot\hat{\mathbf{u}}^* e^{-i\mathbf{k}\cdot\mathbf{r}}|n\rangle\langle vn|I(\varepsilon_a-\varepsilon_v)|ap\rangle}{\varepsilon_a-\varepsilon_v+\varepsilon-\varepsilon_n(1-i0)}, \quad (18)$$

where $I(\Delta)$ is the operator of the electron-electron interaction,

$$I(\Delta) = e^2\alpha_\mu\alpha_\nu\, D^{\mu\nu}(\Delta,\mathbf{x}_{12}), \quad (19)$$

and where $D^{\mu\nu}$ is the photon propagator. In the Feynman gauge, the operator I takes the form

$$I(\Delta) = \frac{\alpha}{4\pi}\,\frac{1-\boldsymbol{\alpha}_1\cdot\boldsymbol{\alpha}_2}{x_{12}}\, e^{i|\Delta|x_{12}}. \quad (20)$$

The summations over n in Eqs. (11)–(18) extend over the complete spectrum of the Dirac equation. The second term on the right-hand side of Eq. (15) corresponds to the $n = v$ contribution excluded from the summation in the first term. The prime on the operator I denotes the derivative with respect to the energy argument. The state v' is the $n = v$ state with the angular momentum projection $\mu_{v'}$. The small imaginary addition to the intermediate-state energies in the energy denominators fixes the position of the energy argument of the electron propagator $G(\mathcal{E})$ with respect to the branch cuts for $|\mathcal{E}| > m$.

We now turn to the physical interpretation of individual diagrams in Fig. 1. The first two graphs represent the effect of the screening of the nuclear charge by the core electron. The corresponding corrections [$\tau^{(1,1)}$ and $\tau^{(1,2)}$] can be regarded as the first-order perturbations of the zero-order amplitude (3) by the screening potential of the core electron,

$$V_{\rm scr}(x) = \alpha\int_0^\infty dy\, y^2\,\frac{1}{\max(x,y)}\left[g_a^2(y)+f_a^2(y)\right], \quad (21)$$

where g_a and f_a are the upper and lower radial components of the core electron state. The screening effect can easily be accounted for to all orders in $1/Z$ by evaluating the zero-order amplitude for an electron in a combination of the nuclear and screening potentials. Such treatment is exactly equivalent to the frozen-core Dirac-Fock method (as the core in our case contains only one electron).

The contribution of diagram 5 in Fig. 1 can be interpreted to represent the electron correlation on the bound-electron wave function (also known as the "relaxation" effect). It can be partly included by standard many-body techniques such as many-body perturbation theory or the multiconfiguration Dirac-Fock method.

The contribution of diagrams 4 and 8 in Fig. 1 contain resonant parts that become prominent when the projectile energy approaches the region where $\varepsilon \approx \varepsilon_v - \varepsilon_a + \varepsilon_n > m$, where ε_n is a Dirac bound-state energy. When the resonance condition is fulfilled, the core electron gets excited into a higher-lying bound state, which corresponds to the standard resonant DR mechanism. In that case, the electron propagator can be replaced by a contribution of the single state responsible for the resonance (the so-called resonance approximation), thus greatly simplifying the problem. In the region far from the resonance, however, the core electron gets "excited" in all possible virtual states of the energy spectrum, so the usage of the full Dirac propagator becomes essential in the description of this process.

Diagrams 3, 6, and 7 in Fig. 1 correspond to other processes with participation of the core electron, in which the full energy spectrum of virtual states is probed. We refer to the contribution of diagrams 3, 4, 6, 7, and 8 as the (off-resonant) DR correction. So, in the present work, the term DR is used to refer to the recombination with an assistance of the second electron, rather than only to the resonant part of this process as is customary. It should be noted that the separation of the total two-electron effect in several parts is to a large extent artificial (e.g., the DR correction defined in this way is not gauge invariant). Its main justification is that the screening and correlation parts are easily accounted for by standard methods, whereas the DR part is not. The sum of all two-electron contributions, however, is gauge invariant and derived rigorously within quantum electrodynamics.

So, we represent the total RR cross section as a sum of four terms,

$$\sigma = \sigma^{(0)} + \sigma_{\rm scr} + \sigma^{(1)}_{\rm corr} + \sigma^{(1)}_{\rm DR}, \quad (22)$$

where $\sigma^{(0)}$ is the zero-order cross section, $\sigma_{\rm scr}$ is the correction induced by the screening potential $V_{\rm scr}$ included to all orders, $\sigma^{(1)}_{\rm corr}$ is the correlation correction induced by $\tau^{(1,5)}$, and $\sigma^{(1)}_{\rm DR}$ is the off-resonant DR contribution induced by $\tau^{(1,3)}$, $\tau^{(1,4)}$, $\tau^{(1,6)}$, $\tau^{(1,7)}$, and $\tau^{(1,8)}$. The screening correction is calculated with the "correct" energy of the emitted photon and, thus, includes the δ_ω correction in Eq. (5). We assume that the projectile energy is far enough from the resonance condition to ensure that the perturbative regime is valid.

III. NUMERICAL EVALUATION

The integration over angular variables in the general formulas of the previous section can be performed by means of the standard Racah algebra, as illustrated in Ref. [13]. The resulting formulas for the zero-order transition amplitude and for the first-order corrections are given in the Appendix. Performing our calculations, we found several sign mistakes in Ref. [13]. Namely, the contributions of Eqs. (A8) and (A9) were accounted for with the opposite sign in that work.

Moreover, the incorrect sign was present in the first term of Eq. (A6) in the case of the capture into the $2p_{1/2}$ state.

The zero-order cross section $\sigma^{(0)}$ and the screening correction $\sigma_{\rm scr}$ were evaluated according to Eqs. (4) and (A2). The radial bound and continuum wave functions were obtained by solving the Dirac equation with an extended-nucleus Coulomb potential and the screening potential of the core electron by using the RADIAL package by Salvat *et al.* [16].

The calculation of the first-order corrections $\sigma^{(1)}_{\rm corr}$ and $\sigma^{(1)}_{\rm DR}$ was more complicated due to a larger number of radial integrations and the summations over the complete spectrum of the Dirac equation. In the evaluation of the $\tau^{(1,5)}$ correction, we employed the dual kinetically balanced B-spline basis set [17] to represent the Dirac spectrum. In most of other cases, we used the analytical representation of the radial Dirac-Coulomb-Green function in terms of Whittaker functions [18]. For simplicity, we used the point-nucleus Green function, since the effect of the finite nuclear size turned out to be negligibly small. In the evaluation of the $\tau^{(1,4)}$ and $\tau^{(1,8)}$ corrections, we used the finite basis set when the energy argument of the Green function was smaller than the electron rest mass ($\mathcal{E} < m$), and the exact Green function otherwise. The Dirac-Coulomb-Green function with $\mathcal{E} > m$ is a complex-valued function and care must be taken in order to choose the appropriate branch of it. The sign of the imaginary part of the Green function is fixed by the sign of the small imaginary addition in the energy denominators of Eqs. (12)–(17) and discussed in detail in Ref. [13].

A problem emerges in the numerical evaluation of the radial integrals when they contain, apart from the Bessel function, two continuum-state wave functions. In this case, the integrand is a rapidly oscillating function that falls off very slowly at large radial distances. In our case, such a situation arises only in the evaluation of the $\tau^{(1,8)}$ correction for projectile energies $\varepsilon > m - \varepsilon_a + \varepsilon_v$. [The problem appears also for the $\tau^{(1,2)}$ correction if it is evaluated perturbatively but not if it is evaluated to all orders.]

Our scheme of evaluating the radial integrals is as follows. First, we introduce the parameter R_1 that represents the distance at which all bound-state wave functions become negligibly small. (Typically, $R_1 = 80/Z$ a.u.) At distances $r > R_1$, all radial integrals with bound-state wave functions reach their asymptotic values, so the problem reduces to the evaluation of one-dimensional integrals of the form

$$\int_{R_1}^{\infty} dr\, r^2\, j_l(\omega r)\, f^i(r)\, \phi^j_\infty(r), \tag{23}$$

where j_l is a spherical Bessel function, f^i is a radial component of the continuum-state Dirac wave function, and ϕ^j_∞ is the irregular solution of the Dirac equation (originating from the Green function). To evaluate these integrals, we introduce a small regulator parameter $\alpha > 0$ and multiply the integrand by $\exp(-\alpha r)$. The regularized integrals are cut off at large distances by a parameter $R_2 \propto 1/\alpha$ and evaluated numerically with Gauss-Legendre quadratures. The typical value of the regulator was $\alpha = 10^{-3}$. We checked that decreasing the regulator by a factor of 10 does not influence our numerical results significantly.

IV. RESULTS AND DISCUSSION

The calculational results for the total cross section of the RR of an electron with an (initially) hydrogenlike uranium are presented in Table I for the capture into the $(1s)^2$, $1s2s$, $1s2p_{1/2}$, and $1s2p_{3/2}$ states. The zero-order cross section, $\sigma^{(0)}$, is calculated with the energy of the emitted photon that includes all known *one-electron* corrections to the energy of the final state; that is, $\omega = \varepsilon - m - \varepsilon_{{\rm io},H}$, where $\varepsilon_{{\rm io},H}$ is the ionization energy of the hydrogenlike ion. The correction due to the screening of the nuclear charge by the core electron, $\sigma_{\rm scr}$, was obtained by reevaluating the zero-order cross section with the wave functions calculated in the presence of the screening potential. The energy of the emitted photon includes all known corrections to the energy of the final state [19]; that is, $\omega = \varepsilon - m - \varepsilon_{\rm io}$, where $\varepsilon_{\rm io}$ is the ionization energy of the heliumlike ion. The correlation correction induced by $\tau^{(1,5)}$ is denoted as $\sigma^{(1)}_{\rm corr}$, and $\sigma^{(1)}_{\rm DR}$ is the off-resonant DR correction induced by $\tau^{(1,3)}$, $\tau^{(1,4)}$, $\tau^{(1,6)}$, $\tau^{(1,7)}$, and $\tau^{(1,8)}$. For the recombination into the excited states, $\sigma^{(1)}_{\rm DR}$ contains a series of the DR resonance peaks in the region of projectile energies $E = 110 - 190$ MeV/nucleon. The behavior of $\sigma^{(1)}_{\rm DR}$ in the vicinity of the peaks is shown in Fig. 2. In the case of recombination into the ground state, $\sigma^{(1)}_{\rm DR}$ does not have any resonances.

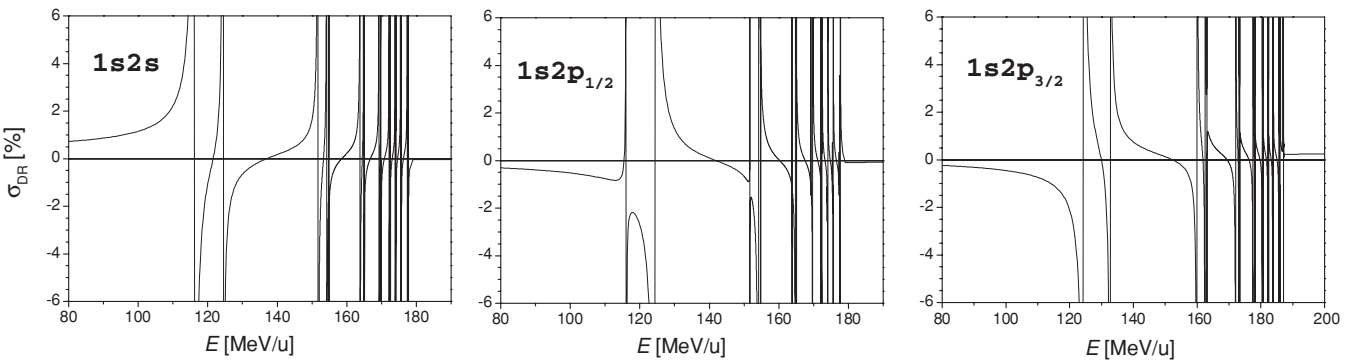

FIG. 2. The contribution of dielectronic recombination $\sigma^{(1)}_{\rm DR}$ for the capture into the $1s2s$, $1s2p_{1/2}$, and $1s2p_{3/2}$ states of the initially hydrogenlike uranium as a function of the projectile energy E, in percent of the zero-order cross section $\sigma^{(0)}$. The threshold energies of the resonant dielectronic recombination for the capture into the $1s2s$, $1s2p_{1/2}$, and $1s2p_{3/2}$ states are $E_0 = 178.6$, 178.4, and 186.7 MeV/nucleon, respectively.

TABLE I. Total cross section of the radiative recombination of an electron into the $(1s)^2$, $1s2s$, $1s2p_{1/2}$, and $1s2p_{3/2}$ states of the initially hydrogenlike uranium for different values of the projectile energy E.[a]

E (MeV/nucleon)	$\sigma^{(0)}$ (barn)	$\sigma_{\rm scr}$ (%)	$\sigma^{(1)}_{\rm corr}$ (%)	$\sigma^{(1)}_{\rm DR}$ (%)	$\sigma^{(0)}$ (barn)	$\sigma_{\rm scr}$ (%)	$\sigma^{(1)}_{\rm corr}$ (%)	$\sigma^{(1)}_{\rm DR}$ (%)
	$(1s)^2$ state				$1s2s$ state			
1	1.588×10^4	−0.850	0.138	−0.703	5.080×10^3	−1.997	−0.232	0.387
2	7.917×10^3	−0.851	0.140	−0.702	2.539×10^3	−1.981	−0.228	0.390
5	3.142×10^3	−0.852	0.146	−0.702	1.013×10^3	−1.936	−0.217	0.396
10	1.550×10^3	−0.854	0.156	−0.701	5.040×10^2	−1.874	−0.201	0.408
25	5.967×10^2	−0.864	0.182	−0.696	1.968×10^2	−1.755	−0.164	0.444
50	2.806×10^2	−0.888	0.217	−0.683	9.315×10	−1.673	−0.124	0.524
75	1.765×10^2	−0.917	0.245	−0.668	5.841×10	−1.652	−0.101	0.669
100	1.254×10^2	−0.949	0.268	−0.650	4.118×10	−1.655	−0.086	1.141
125	9.524×10	−0.981	0.286	−0.634	3.101×10	−1.670	−0.076	−6.124
150	7.559×10	−1.013	0.302	−0.617	2.438×10	−1.690	−0.069	1.635
175	6.188×10	−1.043	0.314	−0.601	1.977×10	−1.712	−0.065	0.443
200	5.184×10	−1.072	0.325	−0.587	1.642×10	−1.735	−0.062	−0.044
250	3.827×10	−1.125	0.341	−0.562	1.192×10	−1.778	−0.060	−0.034
300	2.968×10	−1.170	0.353	−0.542	9.102	−1.817	−0.060	−0.017
400	1.966×10	−1.242	0.369	−0.515	5.879	−1.880	−0.063	0.015
500	1.419×10	−1.292	0.378	−0.499	4.159	−1.926	−0.068	0.034
600	1.084×10	−1.327	0.383	−0.492	3.127	−1.958	−0.074	0.043
700	8.621	−1.350	0.387	−0.495	2.456	−1.980	−0.079	0.045
	$1s2p_{1/2}$ state				$1s2p_{3/2}$ state			
1	7.227×10^3	−2.479	−0.084	−0.045	9.951×10^3	−1.998	0.058	−0.014
2	3.574×10^3	−2.507	−0.087	−0.046	4.888×10^3	−2.034	0.061	−0.015
5	1.384×10^3	−2.589	−0.096	−0.051	1.856×10^3	−2.140	0.067	−0.019
10	6.568×10^2	−2.715	−0.111	−0.060	8.546×10^2	−2.299	0.076	−0.025
25	2.272×10^2	−3.034	−0.147	−0.090	2.737×10^2	−2.682	0.098	−0.049
50	9.209×10	−3.422	−0.195	−0.160	1.006×10^2	−3.119	0.123	−0.106
75	5.138×10	−3.695	−0.232	−0.272	5.205×10	−3.415	0.140	−0.205
100	3.304×10	−3.897	−0.261	−0.520	3.148×10	−3.630	0.152	−0.449
125	2.308×10	−4.053	−0.286	14.715	2.090×10	−3.793	0.160	11.296
150	1.705×10	−4.176	−0.307	−0.666	1.477×10	−3.922	0.166	0.127
175	1.312×10	−4.276	−0.326	−0.222	1.093×10	−4.026	0.171	0.352
200	1.040×10	−4.358	−0.342	−0.047	8.375	−4.113	0.174	0.248
250	7.006	−4.487	−0.369	0.021	5.319	−4.246	0.179	0.297
300	5.041	−4.581	−0.392	0.055	3.646	−4.343	0.181	0.306
400	2.977	−4.712	−0.427	0.071	1.995	−4.473	0.182	0.275
500	1.972	−4.796	−0.455	0.055	1.248	−4.551	0.181	0.222
600	1.410	−4.854	−0.478	0.027	0.853	−4.597	0.179	0.166
700	1.063	−4.895	−0.499	−0.004	0.620	−4.623	0.176	0.111

[a] $\sigma^{(0)}$ is the zero-order cross section, $\sigma_{\rm scr}$ is the screening correction, $\sigma^{(1)}_{\rm corr}$ is the correction due to the electron correlation on the bound electron state, and $\sigma^{(1)}_{\rm DR}$ is the correction due to the dielectronic recombination. All corrections are given in percent of $\sigma^{(0)}$.

Our calculation shows that the effect of the screening of the nuclear charge generally grows for larger projectile energies and the capture into higher excited states, approaching the limit of the complete screening (i.e., the case of the capture by a bare nucleus with the $Z-1$ charge). The effect of the off-resonant DR mechanism is the strongest for the capture into the ground state and for low projectile energies. In this case, the DR contribution is of a size similar to the contribution of the screening effect. We conclude that, for the capture into the ground state, the electron-electron interaction needs to be accounted for rigorously and with inclusion of the off-resonant DR mechanism. Results obtained by an effective one-electron theory or by standard many-body approaches such as the Dirac-Fock method provide only an order-of-magnitude estimate of the two-electron effect in this case. However, for the recombination into the excited states and the projectile energy beyond the DR resonance threshold, the DR correction is much smaller than the screening contribution and can be neglected for most practical purposes. For projectile energies below the threshold, the off-resonant DR mechanism can be important in the vicinity of the peaks, even at relatively large distances from the region of resonance.

In order to illustrate the dependence of the effects studied on the nuclear charge number Z, Table II presents the calculational results for the recombination into the $(1s)^2$ and $1s2s$ states of the initially hydrogenlike tin ($Z=50$).

TABLE II. Total cross section of the radiative recombination of an electron into the $(1s)^2$ and $1s2s$ states of the initially hydrogenlike tin ($Z = 50$) for different values of the projectile energy E.[a]

E (MeV/nucleon)	$\sigma^{(0)}$ (barn)	$\sigma_{\rm scr}$ (%)	$\sigma^{(1)}_{\rm corr}$ (%)	$\sigma^{(1)}_{\rm DR}$ (%)	$\sigma^{(0)}$ (barn)	$\sigma_{\rm scr}$ (%)	$\sigma^{(1)}_{\rm corr}$ (%)	$\sigma^{(1)}_{\rm DR}$ (%)
		$(1s)^2$ state				$1s2s$ state		
1	5.036×10^3	−1.373	0.399	−0.981	1.528×10^3	−3.407	−0.271	0.405
2	2.492×10^3	−1.370	0.419	−0.982	7.598×10^2	−3.345	−0.244	0.399
5	9.669×10^2	−1.362	0.473	−0.983	2.976×10^2	−3.218	−0.174	0.388
10	4.603×10^2	−1.356	0.552	−0.984	1.425×10^2	−3.116	−0.090	0.386
25	1.605×10^2	−1.364	0.721	−0.970	4.931×10	−3.071	0.046	0.532
50	6.568×10	−1.408	0.873	−0.929	1.965×10	−3.133	0.129	0.222
75	3.684×10	−1.455	0.947	−0.887	1.078×10	−3.187	0.152	0.174
100	2.375×10	−1.494	0.985	−0.852	6.835	−3.223	0.153	0.133
125	1.661×10	−1.526	1.003	−0.813	4.718	−3.247	0.144	0.098
150	1.226×10	−1.552	1.010	−0.804	3.447	−3.265	0.131	0.069
175	9.419	−1.575	1.011	−0.796	2.626	−3.277	0.117	0.043
200	7.456	−1.593	1.009	−0.761	2.064	−3.286	0.102	0.022
250	4.996	−1.624	0.999	−0.740	1.367	−3.300	0.073	−0.011
300	3.575	−1.647	0.986	−0.677	0.970	−3.308	0.047	−0.035
400	2.088	−1.680	0.959	−0.618	0.559	−3.317	0.003	−0.063
500	1.372	−1.699	0.935	−0.601	0.364	−3.319	−0.031	−0.080
600	0.974	−1.711	0.914	−0.581	0.257	−3.316	−0.059	−0.089
700	0.732	−1.716	0.896	−0.554	0.192	−3.310	−0.083	−0.094

[a]Notations are the same as in Table I.

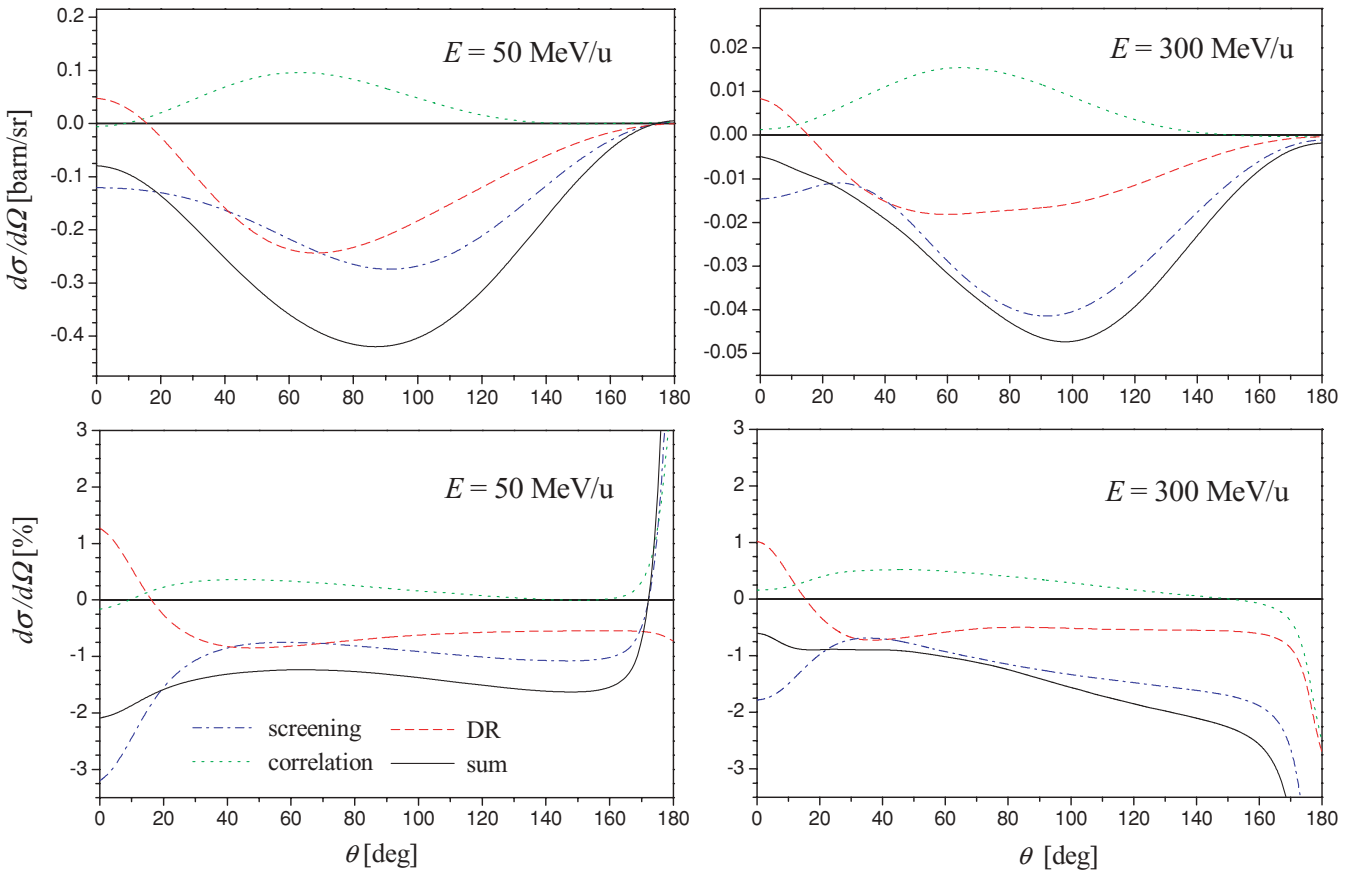

FIG. 3. (Color online) Individual two-electron contributions to the differential cross section of RR into the ground state of the initially hydrogenlike uranium, for two values of the projectile energy, $E = 50$ MeV/nucleon (left column) and 300 MeV/nucleon (right column), as a function of the observation angle θ. The upper graphs represent the absolute contributions to the cross section in barns/sr and the lower graphs represent the relative magnitude of the corrections, in percent of the zero-order cross section $d\sigma^{(0)}$. The dash-dotted (blue) line corresponds to the screening part; the dotted (green) line to the correlation correction; the dashed (red) line to the DR correction; and the solid line to the total two-electron effect.

We observe that the relative contribution of the screening effect is roughly proportional to $1/Z$, as could be expected. It is remarkable that the electron correlation correction, which plays only a minor role for uranium, becomes important for tin in the case of capture into the ground state. The relative contribution of the off-resonant DR mechanism is slightly larger for tin than for uranium, but, in comparison to the screening effect, the DR correction becomes somewhat less significant for lighter ions.

In Fig. 3 we present the results for the differential cross section for the case of the capture into the ground state of uranium, for two values of the projectile energy $E = 50$ and 300 MeV/nucleon, which are typical for the experimental storage ring at GSI. The differential cross section is calculated in the laboratory frame, in which the initially free electron is at rest. We observe that the screening and the DR contributions have different dependences on the observation angle. For the zero angle, they are of opposite sign and significantly cancel each other, whereas for larger angles these two effects amplify each other.

One of the motivations of the present study was a deviation from predictions of one-electron theory reported in the experimental investigation of RR into a hydrogenlike uranium at very small projectile velocities [8]. An effect of about 10% was observed in the experiment, whereas a much smaller contribution on the level of 1–2% was expected from theory [20].

Our *ab initio* calculation demonstrates that the electron-electron interaction affects the RR cross section on the level of about 2% for the projectile energies of several MeV/nucleon, which agrees with previous estimates. For smaller projectile energies, the cross section is well described by the asymptotic behavior $E\,\sigma(E) = \text{const}$, and the relative values of all corrections stay constant. So, our calculation cannot explain the large two-electron effect observed in Ref. [8]. We note, however, that the quantities actually measured in this experiment were not the cross sections but the recombination rates. A consistent interpretation of the experimental results requires a careful consideration of the recombination rates under the experimental conditions. Such a calculation in under way and will be reported elsewhere.

V. SUMMARY

We have performed an investigation of the radiative recombination of an electron with an (initially) hydrogenlike ion. The electron-electron interaction was treated rigorously to the first order in the parameter $1/Z$ and within the screening-potential approximation to the higher orders in $1/Z$. The contribution of the off-resonant dielectronic recombination was studied in detail. It was demonstrated that this mechanism contributes significantly to the total effect of the electron-electron interaction in the case of recombination into the ground state. For the recombination into the excited states, it is significant in the vicinity of the resonance peaks but becomes small for the projectile energies beyond the resonant dielectronic-recombination threshold.

ACKNOWLEDGMENT

The work reported in this paper was supported by the Helmholtz Gemeinschaft (Nachwuchsgruppe Contract No. VH-NG-421).

APPENDIX: CALCULATIONAL FORMULAS

The spherical-wave expansion of the Dirac wave function of an incident electron with a fixed asymptotic momentum is [14]

$$|\mathbf{p}\mu_s\rangle = 4\pi \sum_{\kappa\mu} i^l\, e^{i\Delta_\kappa}\, C^{j\mu}_{lm_l\,\frac{1}{2}\mu_s}\, Y^*_{lm_l}(\hat{\mathbf{p}})\, |\varepsilon\kappa\mu\rangle\,, \qquad \text{(A1)}$$

where $j = |\kappa| - 1/2$, $l = |\kappa + 1/2| - 1/2$, Δ_κ is the phase shift, and $|\varepsilon\kappa\mu\rangle$ is the continuum Dirac wave function with the relativistic angular quantum number κ and the angular momentum projection μ, normalized on the energy scale. After the integration over the angular variables (see Ref. [13] for details), the result for the zero-order amplitude is given by

$$\tau^{(0)}_{\mu_s,\mu_v}(\hat{\mathbf{p}}) = 4\pi \sum_{\kappa} i^l\, e^{i\Delta_k}\, C^{j\mu}_{lm_l\,\frac{1}{2}\mu_s}\, Y^*_{lm_l}(\hat{\mathbf{p}}) \sum_{JL} i^{-1-L}\sqrt{2L+1} \times C^{JM}_{L0\,1\lambda}\,(-1)^{j-\mu}\, C^{JM}_{j_v\mu_v\,j-\mu}\, P_{JL}(\omega,v\varepsilon), \qquad \text{(A2)}$$

where the radial integrals P_{JL} are defined as

$$P_{JL}(\omega,ab) = \int_0^\infty dx\, x^2\, j_L(\omega x)\,[g_b(x)\, f_a(x)\, S_{JL}(\kappa_b, -\kappa_a) - f_b(x)\, g_a(x)\, S_{JL}(-\kappa_b,\kappa_a)]. \qquad \text{(A3)}$$

The angular coefficients $S_{JL}(\kappa_1,\kappa_2)$ are given, for example, by Eqs. (C7)–(C9) of Ref. [21]. The momentum projections μ, M, and m_l in Eq. (A2) are fixed by the selection rules of Clebsch-Gordan coefficients; $\lambda = \pm 1$ corresponds to the circular polarization of the emitted photon. (The cross section does not depend on the sign of λ.)

The one-photon exchange corrections to the transition amplitude $\tau^{(1,i)}$ can be expressed in a form similar to that for the zero-order amplitude, with the radial integrals P_{JL} substituted by their generalizations $\mathcal{F}^{(1,i)}_{JL}$. The results for the functions $\mathcal{F}^{(1,i)}_{JL}$ are

$$\mathcal{F}^{(1,3)}_{JL} = \alpha \sum_n \frac{P_{JL}(\omega,na)}{\varepsilon_a + \varepsilon_v - \varepsilon - \varepsilon_n} \times \frac{(-1)^{J+j_a-j_n}}{2J+1}\, R_J(\varepsilon - \varepsilon_v, va\varepsilon n), \qquad \text{(A4)}$$

$$\mathcal{F}^{(1,4)}_{JL} = \alpha \sum_n \frac{P_{JL}(\omega,an)}{\varepsilon_a - \varepsilon_v + \varepsilon - \varepsilon_n} \times \frac{(-1)^{J+j_a-j_n}}{2J+1}\, R_J(\varepsilon - \varepsilon_v, vn\varepsilon a), \qquad \text{(A5)}$$

$$\mathcal{F}^{(1,5)}_{JL} = \alpha \sum_{\substack{n\neq v\\ \kappa_n=\kappa_v}} \frac{P_{JL}(\omega,n\varepsilon)}{\varepsilon_v - \varepsilon_n} \sum_{L_0} \frac{(-1)^{j_a+j_v+L_0}}{2j_v+1} \times R_{L_0}(\varepsilon_v - \varepsilon_a, avna) + \frac{\alpha}{2}\, P_{JL}(\omega,v\varepsilon) \times \sum_{L_0} \frac{(-1)^{j_a+j_v+L_0}}{2j_v+1}\, R'_{L_0}(\varepsilon_v - \varepsilon_a, avva), \qquad \text{(A6)}$$

$$\mathcal{F}^{(1,6)}_{JL} = \alpha \sum_{\substack{n \\ \kappa_n=\kappa}} \frac{P_{JL}(\omega,vn)}{\varepsilon-\varepsilon_n} \times \sum_{L_0} \frac{(-1)^{j_a+j+L_0}}{2j+1} R_{L_0}(\varepsilon-\varepsilon_a,naa\varepsilon), \quad \text{(A7)}$$

$$\mathcal{F}^{(1,7)}_{JL} = \alpha \sum_{n} \frac{P_{JL}(\omega,na)}{\varepsilon_a+\varepsilon_v-\varepsilon-\varepsilon_n} \sum_{L_0}(-1)^{j_a-j_n+J} \times \begin{Bmatrix} j_v & j & J \\ j_a & j_n & L_0 \end{Bmatrix} R_{L_0}(\varepsilon-\varepsilon_a,av\varepsilon n), \quad \text{(A8)}$$

$$\mathcal{F}^{(1,8)}_{JL} = \alpha \sum_{n} \frac{P_{JL}(\omega,an)}{\varepsilon_a-\varepsilon_v+\varepsilon-\varepsilon_n} \sum_{L_0}(-1)^{j_a-j_n+J} \times \begin{Bmatrix} j & j_v & J \\ j_a & j_n & L_0 \end{Bmatrix} R_{L_0}(\varepsilon_v-\varepsilon_a,vna\varepsilon), \quad \text{(A9)}$$

where R_L is the relativistic generalization of the Slater integral (see Appendix C of Ref. [21]). The prime of R_L in Eq. (A6) denotes the derivative with respect to the energy argument, $R'_L(\varepsilon,abcd) = d/(d\omega)\, R_L(\omega,abcd)|_{\omega=\varepsilon}$.

[1] W. Spies *et al.*, Phys. Rev. Lett. **69**, 2768 (1992).
[2] M. Zimmermann, N. Grün, and W. Scheid, J. Phys. B **30**, 5259 (1997).
[3] M. Tokman *et al.*, Phys. Rev. A **66**, 012703 (2002).
[4] T. Mohamed, D. Nikolić, E. Lindroth, S. Madzunkov, M. Fogle, M. Tokman, and R. Schuch, Phys. Rev. A **66**, 022719 (2002).
[5] T. Stöhlker *et al.*, Phys. Rev. Lett. **73**, 3520 (1994).
[6] T. Stöhlker *et al.*, Phys. Rev. Lett. **79**, 3270 (1997).
[7] T. Stöhlker *et al.*, Phys. Rev. Lett. **82**, 3232 (1999); **84**, 1360(E) (2000).
[8] R. Reuschl, A. Gumberidze, C. Kozhuharov, U. Spillmann, S. Tashenov, T. Stöhlker, and J. Eichler, Phys. Rev. A **77**, 032701 (2008).
[9] S. Fritzsche, A. Surzhykov, and T. Stöhlker, Phys. Rev. A **72**, 012704 (2005).
[10] M. B. Trzhaskovskaya and V. K. Nikulin, Opt. Spectrosc. **95**, 537 (2003) [Opt. Spektrosk. **95**, 580 (2003)].
[11] A. V. Korol, G. F. Gribakin, and F. J. Currell, Phys. Rev. Lett. **97**, 223201 (2006).
[12] A. V. Korol, F. J. Currell, and G. F. Gribakin, J. Phys. B **37**, 2411 (2004).
[13] V. A. Yerokhin, V. M. Shabaev, T. Beier, and J. Eichler, Phys. Rev. A **62**, 042712 (2000).
[14] J. Eichler and W. Meyerhof, *Relativistic Atomic Collisions* (Academic, San Diego, 1995).
[15] V. M. Shabaev, Phys. Rep. **356**, 119 (2002).
[16] F. Salvat, J. M. Fernández-Varea, and W. Williamson Jr., Comput. Phys. Commun. **90**, 151 (1995).
[17] V. M. Shabaev, I. I. Tupitsyn, V. A. Yerokhin, G. Plunien, and G. Soff, Phys. Rev. Lett. **93**, 130405 (2004).
[18] P. J. Mohr, G. Plunien, and G. Soff, Phys. Rep. **293**, 227 (1998).
[19] A. N. Artemyev, V. M. Shabaev, V. A. Yerokhin, G. Plunien, and G. Soff, Phys. Rev. A **71**, 062104 (2005).
[20] S. Fritzsche and A. Surzhykov (unpublished).
[21] V. A. Yerokhin and V. M. Shabaev, Phys. Rev. A **60**, 800 (1999).